Supplemental Material: Ripplonic Lamb Shift for Electrons on Liquid Helium

The Supplemental Material describes the technical details of the calculations carried out in the main text.

I. THE WKB WAVE FUNCTIONS

In this section we describe the analytical approximation for the energies E_n and the eigenfunctions $\psi_n(z)$ of highly excited states of motion normal to the helium surface. For energies $\lesssim 1$ eV and for the distances from the surface $z \gtrsim 1\mathring{A}$, the confining potential above the flat helium surface in Eq. (**??**) has the form

$$V(z) = -\Lambda z^{-1} + eE_\perp z, \qquad \Lambda = e^2 \frac{\epsilon - 1}{4(\epsilon + 1)}, \quad (1)$$

where ϵ is the helium dielectric constant, whereas $V(z) \to \infty$ for $z \to -0$. We note that the effect of the ripplons on the shift of the electron energy levels is accounted for directly, therefore it would be inconsistent to consider the smearing of the helium surface due to the ripplons. However, Eq. (1) has to be modified on the atomic scale, which contributes to the $T = 0$ shift of the electron energy levels [1–5], as indicated in the main text.

We change to dimensionless length, energy, and pressing field,

$$\zeta = z/r_B, \qquad \varepsilon_n = E_n/R, \qquad F = (eE_\perp r_B)/R, \quad (2)$$

($r_B = \hbar^2/\Lambda m$ and $R = \hbar^2/2mr_B^2$ are the localization length of the ground state and the electron binding energy for $E_\perp = 0$). We will assume that the dimensionless force is small, $F \lesssim 1$; in the experiment discussed in this paper $F \sim 0.1$.

In the variables (2) the Schrödinger equation for the motion normal to the surface becomes

$$\left[-\frac{d^2}{d\zeta^2} - \frac{2}{\zeta} + F\zeta\right]\psi_n(\zeta) = \varepsilon_n \psi_n(\zeta) \quad (3)$$

with the boundary condition $\psi_n(0) = 0$.

For large energies $\varepsilon_n \gg 1$ and not too small ζ the solution can be sought in the WKB form

$$\psi_n(\zeta) = \frac{C_n}{\sqrt{p(\zeta, \varepsilon_n)}} \sin\left[S(\varepsilon_n) - \int_0^\zeta p(\zeta', \varepsilon_n) d\zeta' + \frac{\pi}{4}\right],$$
$$S(\varepsilon_n) = \int_0^{\zeta_n} p(\zeta', \varepsilon_n) d\zeta', \quad (4)$$

where $p(\zeta, \varepsilon) = [\varepsilon + 2/\zeta - F\zeta]^{1/2}$ is the scaled classical momentum of motion in the z-direction and C_n is the normalization constant, which we set to be a real number. The value of ζ_n is given by equation $p(\zeta_n, \varepsilon_n) = 0$; for large ε_n we have $\zeta_n \approx F^{-1}\varepsilon_n + 2\varepsilon_n^{-1} \gg 1$.

The WKB approximation breaks down for small ζ, because the confining potential is singular at $\zeta \to 0$. For the WKB to apply, the de Broglie wavelength should be small compared to the distance on which it changes. This means that Eq. (4) applies for $\zeta \gg \varepsilon_n^{-3/4}$.

For small ζ, where $F\zeta \ll \varepsilon + 2/\zeta$, we can disregard the term $F\zeta$ in Eq. (3). The solution of this equation then becomes

$$\psi_n(\zeta) = \tilde{C}_n \zeta e^{-i\varepsilon_n^{1/2}\zeta} {}_1F_1\left(i\varepsilon_n^{-1/2} + 1, 2, 2i\varepsilon_n^{1/2}\zeta\right) + \text{c.c.}, \quad (5)$$

where ${}_1F_1$ is the confluent hypergeometric function and $\tilde{C}_n$ is a constant. We will see that $\tilde{C}_n$ can be assumed real, in which case the term $\propto {}_1F_1$ and its complex conjugate are equal.

The solutions (4) and (5) should match in the range where $\varepsilon_n^{3/4}\zeta \gg 1$ and at the same time $F\zeta \ll \varepsilon_n + 2/\zeta$. In the considered case of large ε_n, both solutions should apply in the range $\varepsilon_n/F \gg \zeta \gg \varepsilon_n^{-1/2}$. For $\varepsilon_n^{1/2}\zeta \gg 1$ we have

$${}_1F_1\left(i\varepsilon_n^{-1/2} + 1, 2, 2i\varepsilon_n^{1/2}\zeta\right) \approx [1/\Gamma(1 + i\varepsilon_n^{-1/2})]$$
$$\times \exp[2i\varepsilon_n^{1/2}\zeta + (i\varepsilon_n^{-1/2} - 1)\log(2i\varepsilon_n^{1/2}\zeta)],$$

so that, assuming $\tilde{C}_n$ to be real, we have in this range from Eq. (5)

$$\psi_n(\zeta) \approx \tilde{C}_n \varepsilon_n^{-1/2} e^{-\pi/2\varepsilon_n^{1/2}} \times \sin\left\{\varepsilon_n^{1/2}\zeta + \varepsilon_n^{-1/2}[\ln(2\varepsilon_n^{1/2}\zeta) + \gamma]\right\}, \quad (6)$$

(γ is the Euler constant), whereas Eq. (4) gives

$$\psi_n(\zeta) \approx C_n \varepsilon_n^{-1/4} \sin\left\{S(\varepsilon_n) + \frac{\pi}{4} - \varepsilon_n^{1/2}\zeta - \varepsilon_n^{-1/2}[1 + \ln(2\varepsilon_n\zeta)]\right\} \quad (7)$$

By comparing Eqs. (6) and (7), we obtain

$$S(\varepsilon_n) = \pi\left(n - \frac{1}{4}\right) + \varepsilon_n^{-1/2}(1 - \gamma + \ln \varepsilon_n^{1/2}) \quad (8)$$

with integer n; $\tilde{C}_n = (-1)^{n+1} C_n \varepsilon_n^{1/4} \exp(\pi/2\varepsilon_n^{1/2})$.

The classical action $S(\varepsilon)$ can be found for small F/ε^2 and $\varepsilon \gg 1$, where the image potential can be considered a perturbation. The image-potential induced correction is nonanalytic in ε,

$$S(\varepsilon) \approx \frac{2\varepsilon^{3/2}}{3F} + \varepsilon^{-1/2}\log(c_\varepsilon \varepsilon^2/F), \qquad F/\varepsilon^2 \ll 1, \quad (9)$$

where constant $c_\varepsilon \approx 20$ is estimated by interpolating the numerical value of $S(\varepsilon)$. Equations (8) and (9) give the

energy spectrum of the excited states with logarithmic corrections from the image potential, $\varepsilon_n \approx \varepsilon_n^{(0)} + \varepsilon_n^{(1)}$,

$$\varepsilon_n^{(0)} = \left[(3\pi F/2)\,(n-1/4)\right]^{2/3},$$
$$\varepsilon_n^{(1)} = -\frac{F}{\varepsilon_n^{(0)}}\left[\frac{3}{2}\ln\varepsilon_n^{(0)} - 1 + \gamma + \ln(c_\varepsilon/F)\right]. \qquad (10)$$

To the leading order in ε_n^{-1}, the normalization constant C_n can be calculated disregarding the image potential. From Eq. (4), $C_n \approx F^{1/2}\varepsilon_n^{-1/4}$.

For very large ε_n one can disregard the image potential in Eq. (3) and assume that the electrons are in a triangular well. The solution $\psi_n(\zeta)$ can be sought in terms of the Airy functions as $\mathrm{Ai}\big(F^{1/3}(\zeta - F^{-1}\varepsilon_n)\big)$, with ε_n determined by the condition $\psi_n(0) = 0$. This gives asymptotically the same leading term $\varepsilon_n^{(0)}$ in the expression for the energy, ε_n. The correction from the image potential can be calculated as $-2\langle\psi_n|\zeta^{-1}|\psi_n\rangle$; the result is close to Eq. (10) for $\varepsilon_n^{(1)}$.

In order to compare the results with the experiment [6, 7], we performed a detailed numerical study of the energies and the wave functions for the field $E_\perp = 106$ V/cm used in the experiment. We calculated the energies E_n as well as the matrix elements of the momentum p_z (and of the electrostatic interaction, see below) for $n \le 30$ by numerically solving the Schrödinger equation (3). For larger n, one can use Eq. (5) to describe the wave functions in the region of small $\zeta \lesssim 1$, which contribute to the overlap integrals $\langle n|p_z|n_1\rangle$ with $n_1 \sim 1$. Expression (5) for ψ_n was corrected by multiplying it by an extra factor $\exp(iF\zeta^2/4\varepsilon_n^{1/2})$. This factor accounts for the field-induced term in the WKB expression (4), which was dropped in Eq. (7) to match Eq. (5), which refers to the limit $F\zeta^2 \to 0$.

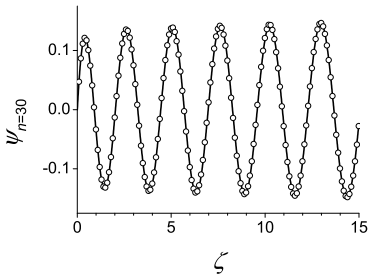

FIG. 1. Solid line: the analytical expression (5) for the wave function of the level $n = 30$ at small distance from the surface; the expression has been corrected by the WKB factor $\exp(iF\zeta^2/4\varepsilon_n^{1/2})$. The numerical results are shown by dots. The data refers to $E_\perp = 106$ V/cm, the dimensionless energy of the level is $\varepsilon_{30} = 6.57$

We found that for $n \gtrsim 20$ functions $\psi_n(\zeta)$ modified this way are in a very good agreement with the numerically calculated wave functions in the whole region $\zeta \ll \varepsilon_n/F$, see Fig.1. The values of the matrix elements $\langle n|p_z|n_1\rangle$ calculated with such $\psi_n(\zeta)$ for $n_1 = 1, 2$ are in a very good agreement with the numerical values, too, see Table I. Therefore in the numerical calculations for large n we used these functions. The matrix elements $\langle n|p_z|n_1\rangle$ become close to those for ψ_n calculated in the triangular well approximation for $n \gtrsim 10^4$.

TABLE I. Values of the scaled matrix elements $\pi_{1n} = (i/\hbar)r_B\langle n|p_z|1\rangle$ and $\pi_{2n} = (i/\hbar)r_B\langle n|p_z|2\rangle]$ calculated for $E_\perp = 106$ V/cm and for large n using Eq. (5) with the WKB correcting factor (see Fig. 1) and the approximation of a triangular potential well. The wave functions $\psi_{1,2}$ are calculated numerically. For comparison, the numerical solutions of Eq. (3) for n = 30 give $\pi_{1n} = 0.0662$ and $\pi_{2n} = 0.0415$.

n	Equation (3)		Triangular well	
	π_{1n}	$[\pi_{2n}]$	π_{1n}	$[\pi_{2n}]$
30	0.0663	[0.0415]	0.0740	[0.0443]
10^2	0.0347	[0.0199]	0.0419	[0.0239]
10^3	0.0091	[0.0049]	0.0104	[0.0056]
10^4	0.0021	[0.0011]	0.0023	[0.0012]
10^5	0.0005	[0.0003]	0.0005	[0.0003]

As a test of the accuracy of our numerical calculation we checked the convergence of the sums

$$\sum_{n'\le n_{\max}} |\langle n'|p_z|n\rangle|^2 \to \langle n|p_z^2|n\rangle,\ n_{\max}\to\infty,$$
$$\sum_{n'\le n_{\max},\, E_{n'}\ne E_n} \frac{|\langle n'|p_z|n\rangle|^2}{(E_n - E_{n'})} \to -m/2,\ n_{\max}\to\infty. \qquad (11)$$

The results presented in Fig. 2 show slow, but consistent convergence.

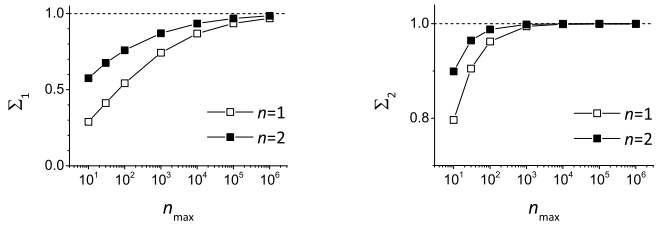

FIG. 2. The convergence of the numerically evaluated sums (11) relevant for finding the energy shift of the states $n = 1$ and $n = 2$; $\Sigma_1 = \sum_{n'\le n_{\max}} |\langle n'|p_z|n\rangle|^2/\langle n|p_z^2|n\rangle$ and $\Sigma_2 = (2/m)\sum_{n'\le n_{\max}} |\langle n'|p_z|n\rangle|^2/(E_{n'} - E_n)$. The data refer to the pressing field $E_\perp = 106$ V/cm used in the experiment.

As expected from the estimate that led to Eq. (8) of the main text, the matrix elements $\langle n|p_z|n_1\rangle$ fall off approximately as $n^{-2/3}$ for $n \gg 1$ and $n_1 \sim 1$. Therefore it was necessary to sum over a large number of the virtual states in Eq. (7) of the main text. In this equation the summation index is n', and in Eq. (11) and below we refer to sums over n' for given n. If the sum over n' in Eq. (7)

of the main text is limited to $n' \leq 10^5$, the energy $E_{n'}$ is ≤ 0.98 eV for the considered $E_\perp = 106$ V/cm, which is on the boundary of the approximation of an infinite potential barrier at the helium surface.

The shape of the electron barrier $V(z)$ on the helium surface for energies > 1 eV and the form of the electron wave functions for the states with energies > 1 eV are not known. Also, the shape of the wave function of the low lying states at distances $< 1\mathring{A}$ from the surface is not known either. However, we can find the contribution of the highly excited states to the level shift using the sum rules (11).

To see how it comes about we note first that, in the T-dependent term in Eq. (7) of the main text for the level shift, the sum over the ripplon wave vectors $\mathbf{q}$ is limited to $q \lesssim q_T$. Therefore, for temperatures $T \lesssim 0.8$ K, as seen from Fig. 1(b) of the main text, $\Delta_{\mathbf{p},\mathbf{q},\alpha} < 0.1$ eV. If $E_{n_{\max}} - E_n \gg \Delta_{\mathbf{p},\mathbf{q},\alpha}$, in the terms with $n' > n_{\max}$ in Eq. (7) of the main text one can expand the denominator in $\Delta_{\mathbf{p},\mathbf{q},\alpha}/(E_n - E_{n'})$. The sums over $n' > n_{\max}$ for the terms of the zeroth and first order are then given by the above sum rules with the subtracted terms for $n' < n_{\max}$. Therefore, once the summation in Eq. (7) of the main text has been done for $n < n_{\max}$, the overall level shift is known from the sum rules to the first order in the parameter $\delta_{\max} = \Delta_{\mathbf{p},q_T,\alpha}/(E_{n_{\max}} - E_n)$ irrespective of the form of the barrier $V(z)$. The second-order term in $\delta_{\max}$ can be easily found also using the sum rule for $|\langle n|p_z|n'\rangle|^2/(E_n - E_{n'})^2$.

For $E_\perp = 106$ V/cm and $n_{\max} = 10^5$, we have $\delta_{\max} \sim 0.1$. Given that the sum rules hold very well for the wave functions we have found, we could therefore extend the summation in Eq. (7) to $n' \to \infty$ using these wave functions. This is the procedure used to obtain the energy shift in Fig. 2 of the main text.

II. CONTRIBUTION OF THE ELECTROSTATIC COUPLING

Ripplon-induced warping of the helium surface leads to a change of the electron image potential. The energy of the electron-ripplon coupling is the change of the polarization energy of liquid helium in the electric field of the electron. For the electron located at $\mathbf{r}$ it has the form [8, 9]

$$V^{\rm pol}(\mathbf{r},z) = -\frac{\Lambda}{\pi}\int d\mathbf{r}_1 \int_0^{\xi(\mathbf{r}_1)-\xi(\mathbf{r})} dz_1 \times [(\mathbf{r}-\mathbf{r}_1)^2 + (z-z_1)^2]^{-2}, \qquad (12)$$

where $\Lambda = e^2(\epsilon_{\rm He}-1)/8$ ($\epsilon_{\rm He} \approx 1.057$ is the helium dielectric constant and we disregard the terms of higher order in $\epsilon_{\rm He} - 1$).

Because the ratio $\langle\xi^2\rangle^{1/2}/r_B$ is small, one can expand the energy (12) to the second order in $\xi(\mathbf{r})$. One should also take into account another part of the electrostatic energy, which is the energy of the electron in the transverse field $E_\perp$. This energy changes when the electron position is shifted by $\xi(\mathbf{r})$. The expression for the total electrostatic part of the electron-ripplon coupling energy then reads

$$\hat{H}_i^{\rm el} = \sum_{\mathbf{q}} V_{\mathbf{q}}^{(1)}(z)\xi_{\mathbf{q}} e^{i\mathbf{q}\mathbf{r}} + \sum_{\mathbf{q}_1,\mathbf{q}_2} V_{\mathbf{q}_1,\mathbf{q}_2}^{(2)}(z)\xi_{\mathbf{q}_1}\xi_{\mathbf{q}_2} e^{i(\mathbf{q}_1+\mathbf{q}_2)\mathbf{r}}. \qquad (13)$$

Here, $\xi_{\mathbf{q}} = Q_q(b_{\mathbf{q}} + b_{-\mathbf{q}}^\dagger)$, see Eq. (2) of the main text. Functions $V_{\mathbf{q}}^{(1)}$ and $V_{\mathbf{q}_1\mathbf{q}_2}^{(2)}$ describe one- and two-ripplon coupling, respectively. They are given in Refs. 8–10,

$$V_{\mathbf{q}}^{(1)}(z) = \Lambda z^{-2}[1 - qzK_1(qz)] + eE_\perp,$$
$$V_{\mathbf{q}_1,\mathbf{q}_2}^{(2)}(z) = -\frac{\Lambda}{z^3} + \frac{\Lambda}{2z}\left[q_1^2K_2(q_1z) + q_2^2K_2(q_2z) - (\mathbf{q}_1+\mathbf{q}_2)^2K_2\left(|\mathbf{q}_1+\mathbf{q}_2|z\right)\right] \qquad (14)$$

$K_{1,2}(x)$ are the modified Bessel functions. In the last term in Eq. (14) for $V_{\mathbf{q}_1\mathbf{q}_2}^{(2)}$ one should replace $(\mathbf{q}_1 + \mathbf{q}_2)^2K_2\left(|\mathbf{q}_1+\mathbf{q}_2|z\right)$ with $2/z^2$ for $\mathbf{q}_1 = -\mathbf{q}_2$.

The expansion of $V^{\rm pol}(\mathbf{r},z)$ in $\xi(\mathbf{r})$ breaks down for very small z. In this range the major contribution to the integral over $\mathbf{r}_1$ in Eq. (12) comes from small $|\mathbf{r}_1 - \mathbf{r}|$. For such $\mathbf{r}_1$, and assuming that $\xi(\mathbf{r})$ is smooth, one can expand $\xi(\mathbf{r}_1) - \xi(\mathbf{r}) \approx |\boldsymbol{\nabla}\xi(\mathbf{r})| \cdot |\mathbf{r}_1 - \mathbf{r}| \cdot \cos\phi$ where ϕ is the angle between $\boldsymbol{\nabla}\xi(\mathbf{r})$ and $\mathbf{r}_1 - \mathbf{r}$. One can then integrate over $|\mathbf{r}_1 - \mathbf{r}|$ for a given ϕ and z_1, then over z_1, and ultimately over ϕ. For $z \to 0$, to the leading order in $1/z$ the result reads

$$V^{\rm pol}(\mathbf{r},z) \approx -\frac{\Lambda}{2\pi z}\int_{-\pi/2}^{\pi/2} d\phi \frac{\pi - 2\arctan y(\mathbf{r},\phi)}{y(\mathbf{r},\phi)}, \quad y(\mathbf{r},\phi) = [|\boldsymbol{\nabla}\xi(\mathbf{r})|\cos\phi]^{-1} \qquad (15)$$

For small $|\boldsymbol{\nabla}\xi(\mathbf{r})|$, this expression is $\propto [\boldsymbol{\nabla}\xi(\mathbf{r})]^2$, to the leading order in $|\boldsymbol{\nabla}\xi(\mathbf{r})|$. It then coincides with the asymptotic form of $H_i^{\rm el}$ for small z, where the major contribution to $H_i^{\rm el}$ comes from $V_{\mathbf{q}_1,\mathbf{q}_2}^{(2)}(z)$. Numerically, approximating Eq. (15) by the term $\propto [\boldsymbol{\nabla}\xi(\mathbf{r})]^2$ works well in a broad range of $|\boldsymbol{\nabla}\xi(\mathbf{r})|$; even for $|\boldsymbol{\nabla}\xi(\mathbf{r})| = 0.7$ the difference with the full expression (15) is $< 10\%$, and it decreases fast with the decreasing $|\boldsymbol{\nabla}\xi(\mathbf{r})|$.

The assumption of the smoothness of $\xi(\mathbf{r})$ used in Eq. (15) requires that the root mean square displacement $\langle\xi^2(\mathbf{r})\rangle^{1/2}$ largely exceed the typical length on which $\xi(\mathbf{r})$ changes. If we limit the ripplon wave numbers to $q_c = 10^8$ cm^{-1}, for the $T = 0$ fluctuations we have $q_c\langle\xi^2(\mathbf{r})\rangle_{T=0}^{1/2} \sim 1.5$, cf. Fig. 1(c) of the main text. This shows that Eq. (15) is a good approximation for small $|\boldsymbol{\nabla}\xi(\mathbf{r})|$, whereas for $|\boldsymbol{\nabla}\xi(\mathbf{r})| \gtrsim 1$ in the expansion of $\xi(\mathbf{r}_1) - \xi(\mathbf{r})$ in Eq. (12) one should take into account higher-order terms in $\mathbf{r}_1 - \mathbf{r}$. They lead to $V^{\rm pol}(\mathbf{r},z)$ increasing even slower than z^{-1} with the decreasing z, for very small z.

From Eq. (15), the region of small z does not contribute appreciably to the matrix elements of $V^{\rm pol}(\mathbf{r},z)$ on the wave functions $\psi_n(z)$, which are $\propto z$ for small z. In the whole region $|\boldsymbol{\nabla}\xi(\mathbf{r})| \leq 1$ the integral of $z^2 V^{\rm pol}(\mathbf{r},z)$ over the range $z \lesssim \langle\xi^2(\mathbf{r})\rangle_{T=0}^{1/2} \sim 10^{-8}$ cm gives an extremely small contribution to the level shift, $\lesssim R\langle\xi^2(\mathbf{r})\rangle_{T=0}/r_B^2 \sim 10^{-3}R$ (we keep only the $T=0$ terms in this estimate, since only such terms are essential for large ripplon wave numbers). At the same time, for not too small z the coupling energy (12) is nonsingular and can be expanded in $\xi(\mathbf{r})$. This justifies using Eqs. (13) and (14) to describe the electrostatic electron-ripplon coupling.

The direct two-ripplon coupling $\propto V^{(2)}_{\mathbf{q}_1,\mathbf{q}_2}(z)$ leads to a shift of the energy levels already in the first order of the perturbation theory. From Eq. (13), for an nth level the shift is

$$\Delta\tilde{E}_n^{(2)} = \sum_{\mathbf{q}} \langle n|V^{(2)}_{\mathbf{q},-\mathbf{q}}(z)|n\rangle |Q_q|^2 (2\bar{n}_q + 1).$$

The terms linear in $\xi_{\mathbf{q}}$ give a shift when taken to the second order. This shift is determined by the matrix elements of the sum of the kinematic interaction $\hat{H}_i^{(1)}$ [Eq. (3) of the main text] and the linear in $\xi_{\mathbf{q}}$ terms in Eq. (13). To calculate the sum over the intermediate electron states, one can use the Bethe trick, Eq. (6) of the main text. One can then use the relation $i[p_z, V^{(1)}_{\mathbf{q}}(z)] = \hbar V^{(2)}_{\mathbf{q},-\mathbf{q}}(z)$, which follows from Eq. (14), to show that the shift $\Delta\tilde{E}_n^{(2)}$ cancels out (in the calculation one should also use the completeness condition $\sum_{n'}\langle n|\hat{A}|n'\rangle\langle n'|\hat{B}|n\rangle = \langle n|\hat{A}\hat{B}|n\rangle$ that holds for any operators $\hat{A},\hat{B}$). The full expression for the level shift due to the electrostatic electron-ripplon coupling, which also includes the cross term from the electrostatic and kinematic coupling, is

$$\Delta E^{\rm pot}_{n\mathbf{p}} = \hbar \sum_{\mathbf{q},\alpha} \mathcal{N}_{q\alpha} \sum_{n'} (E_n - E_{n'} - \Delta_{\mathbf{p},\mathbf{q},\alpha})^{-1} \left[\hbar \left|\langle n'|V^{(1)}_{\mathbf{q}}(z)|n\rangle\right|^2 - 2(E_n - E_{n'}) {\rm Im}\, \langle n|p_z|n'\rangle\langle n'|V^{(1)}_{\mathbf{q}}(z)|n\rangle\right], \quad (16)$$

where $\mathcal{N}_{q\alpha} = |Q_q|^2 \left[\bar{n}_q + (1+\alpha)/2\right]/\hbar^2$, cf. the main text; $\Delta_{\mathbf{p},\mathbf{q},\alpha}$ is defined in the main text below Eq. (5). The level shift (16) should be added to the purely kinematic shift given by Eq. (7) of the main text to describe the full level shift due to the electron-ripplon coupling. Note that the term with $n' = n$ gives the polaronic shift due to virtual processes within the same subband of motion normal to the surface, see [8, 11, 12]. The term quadratic in the pressing field $E_\perp$, which gives the major contribution to this shift for large $E_\perp$ [12], is independent of the subband number n and drops out from the expression for the frequency of inter-subband transitions, which is of the central interest for this paper.

A numerical calculation shows that, for typical pressing fields $E_\perp \lesssim 300$ V/cm, the $T=0$ level shift described by Eq. (16) is much smaller than the $T=0$ kinematic shift discussed in the main text. For $E_\perp = 106$ V/cm (the field used in the experiment discussed in the main text), the $T=0$ term in the sum (16) for $n=1$ and $q \gtrsim 10^7$ cm^{-1} is an order of magnitude smaller than the corresponding term in Eq. (7) of the main text. The $T=0$ shift given by Eq. (16) is a part of the small deviation from the simple model of noninteracting electrons above the flat helium surface. Such deviation has not been measured in the experiment, and it is not easy to measure. This paper shows that the deviation is small without using adjustable parameters or extra approximations.

III. TWO-RIPPLON SCATTERING

As indicated in the main text, the two-ripplon coupling can provide an important contribution to inelastic electron scattering. This is a consequence of the possibility to scatter into ripplons with large wave numbers q, q' while keeping the total ripplon momentum $\hbar(\mathbf{q}+\mathbf{q}')$ small, of the order of the electron thermal momentum or the reciprocal quantum localization length in a magnetic field multiplied by $\hbar$. The scattering rate is determined by the transition matrix elements calculated for the same total energy and the same total momentum of the electron-ripplon system in the initial and finite states. These matrix elements (the vertex, in terms of the diagrams) are given by the direct two-ripplon coupling in the first order and the single-ripplon coupling in the second order of the perturbation theory.

If only the direct two-ripplon coupling was kept in the analysis of inelastic scattering, this would lead to a very high scattering rate. For example, the rate of transitions from the bottom of the first excited subband ($n=2, \mathbf{p}=0$) to the lowest subband ($n=1$) due to the kinematic coupling $\hat{H}_i^{(2)}$ [Eq. (3) of the main text] would be $\gtrsim 10^8$ s^{-1}. This is orders of magnitude higher than in the existing experimental data. However, as in the case of the electron energy shift, the major part of the direct coupling is compensated by the linear in $\xi(\mathbf{r})$ coupling $\hat{H}_i^{(1)}$. To find this compensation, one can use again the Bethe trick.

We consider an electron transition from the initial

state $|n_i, \mathbf{p}_i, \{n(\mathbf{q})\}\rangle$ to the final state $|n_f, \mathbf{p}_f, \{n'(\mathbf{q})\}\rangle$, where $|\{n(\mathbf{q})\}\rangle$ is the ripplon wave function in the occupation number representation. To the first order in $\hat{H}_i^{(2)}$ and to the second order in $\hat{H}_i^{(1)}$, the matrix element $\mathcal{M}_{if}^{\rm kin}(\mathbf{q}_1, \mathbf{q}_2)$ of the kinematic coupling, which describes a two-ripplon transition with emission or absorption of ripplons with wave vectors $\mathbf{q}_1$ and $\mathbf{q}_2$, has the form

$$\mathcal{M}_{if}^{\rm kin}(\mathbf{q}_1, \mathbf{q}_2) = g_{\alpha\beta}\hbar^{-2}Q_{q_1}Q_{q_2}\left[\langle n_f|p_z^2|n_i\rangle(E_{n_i}-E_{n_f}) - \sum_{n'}\langle n_f|p_z|n'\rangle\langle n'|p_z|n_i\rangle(E_{n_i}-E_{n'})\right.$$
$$\left.\times\left(L_{n_in'}^{\alpha_1\alpha_2}(\mathbf{q}_1,\mathbf{q}_2) + L_{n_in'}^{\alpha_2\alpha_1}(\mathbf{q}_2,\mathbf{q}_1)\right)\right], \quad L_{n_in'}^{\alpha_1\alpha_2}(\mathbf{q}_1,\mathbf{q}_2) = \Delta_{\mathbf{p}_i+\hbar\mathbf{q}_1,\mathbf{q}_2,\alpha_2}/(E_{n_i}-E_{n'}-\Delta_{\mathbf{p}_i,\mathbf{q}_1,\alpha_1}) \tag{17}$$

Here, the subscripts $\alpha_{1,2}$ indicate whether the transition is accompanied by ripplon emission ($\alpha_1 = \alpha_2 = 1$), absorption ($\alpha_1 = \alpha_2 = -1$), or scattering ($\alpha_1 = -\alpha_2 = \pm 1$). Factor $g_{\alpha_1\alpha_2} \equiv g_{\alpha_1\alpha_2}(\mathbf{q}_1, \mathbf{q}_2)$ is determined by the initial ripplon occupation numbers, $g_{\alpha_1,\alpha_2}(\mathbf{q}_1, \mathbf{q}_2) = \{[n(-\alpha_1\mathbf{q}_1) + (1+\alpha_1)/2][n(-\alpha_2\mathbf{q}_2) + (1+\alpha_2)/2]\}^{1/2}$. In the final ripplon state $|\{n'(\mathbf{q})\}\rangle$ the occupation numbers of ripplons with the wave vectors $-\alpha_1\mathbf{q}_1$ and $-\alpha_2\mathbf{q}_2$ are changed by α_1 and α_2, respectively, compared to the state $|\{n(\mathbf{q})\}\rangle$. In Eq. (17) we took into account that the final and initial energy of the electron-ripplon system is the same as is also the total in-plane momentum, $\mathbf{p}_f = \mathbf{p}_i + \hbar(\mathbf{q}_1 + \mathbf{q}_2)$.

One can similarly calculate the contribution of the electrostatic electron-ripplon coupling to the matrix element of two-ripplon scattering. An important cancellation of the terms with large ripplon momenta occurs in this case, too. To the first order in the direct electrostatic two-ripplon coupling and to the second order in the one-ripplon electrostatic coupling and the cross-term with the one-ripplon kinematic coupling, using Eq. (14) we obtain for the matrix element of the same transition as in Eq. (17) the expression

$$\mathcal{M}_{if}^{\rm pot}(\mathbf{q}_1, \mathbf{q}2) = g_{\alpha_1\alpha_2}Q_{q_1}Q_{q_2}\left\{\left\langle n_f\left|\Lambda\left[\frac{2}{z^3} - \frac{(\mathbf{q}_1+\mathbf{q}_2)^2}{z}K_2(|\mathbf{q}_1+\mathbf{q}_2|z)\right] - i\left[\frac{E_{n_f}-E_{n_i}}{\hbar\Delta_{\mathbf{p}_i,\mathbf{q}_1,\alpha_1}}p_zV_{\mathbf{q}_1}^{(1)} + (\mathbf{q}_1 \leftrightharpoons \mathbf{q}_2)\right]\right|n_i\right\rangle\right.$$
$$\left. + \left[\frac{\langle n_f|V_{\mathbf{q}_2}^{(1)}|n'\rangle\langle n'|V_{\mathbf{q}_1}^{(1)} - (i/\hbar)(E_{n_i}-E_{n'})p_z|n_i\rangle}{E_{n_i}-E_{n'}-\Delta_{\mathbf{p}_i,\mathbf{q}_1,\alpha_1}} - i\frac{(E_{n_i}-E_{n'})\Delta_{\mathbf{p}_i+\hbar\mathbf{q}_1,\mathbf{q}_2,\alpha_2}\langle n_f|p_z|n'\rangle\langle n'|V_{\mathbf{q}_1}^{(1)}|n_i\rangle}{\hbar\Delta_{\mathbf{p}_i,\mathbf{q}_1,\alpha_1}(E_{n_i}-E_{n'}-\Delta_{\mathbf{p}_i,\mathbf{q}_1,\alpha_1})} + (\mathbf{q}_1 \leftrightharpoons \mathbf{q}_2)\right]\right\}. \tag{18}$$

Here $V_{\mathbf{q}}^{(1)}$ is a shorthand for $V_{\mathbf{q}}^{(1)}(z)$ and "$+(\mathbf{q}_1 \leftrightharpoons \mathbf{q}_2)$" means adding the same expression with the interchanged $\{\mathbf{q}_1, \alpha_1\}$ and $\{\mathbf{q}_2, \alpha_2\}$; function g_{α_1,α_2} is defined below Eq. (17). Numerical calculations of the relaxation rate based on Eqs. (17) and (18) are beyond the scope of the present paper.

[1] C. C. Grimes, T. R. Brown, M. L. Burns, and C. L. Zipfel, Phys. Rev. B **13**, 140 (1976).
[2] F. Stern, Phys. Rev. B **17**, 5009 (1978).
[3] M. V. Rama Krishna and K. B. Whaley, Phys. Rev. B **38**, 11839 (1988).
[4] E. Cheng, M. W. Cole, and M. H. Cohen, Phys. Rev. B **50**, 1136 (1994).
[5] M. H. Degani, G. A. Farias, and F. M. Peeters, Phys. Rev. B **72**, 125408 (2005).
[6] E. Collin, W. Bailey, P. Fozooni, P. G. Frayne, P. Glasson, K. Harrabi, M. J. Lea, and G. Papageorgiou, Phys. Rev. Lett. **89**, 245301 (2002).
[7] E. Collin, W. Bailey, P. Fozooni, P. G. Frayne, P. Glasson, K. Harrabi, and M. J. Lea, ArXiv e-prints (2017), 1707.02119.
[8] M. W. Cole, Phys. Rev. B **2**, 4239 (1970).
[9] V. Shikin and Y. Monarkha, J. Low Temp. Phys. **16**, 193 (1974).
[10] M. I. Dykman, P. Platzman, and P. Seddighrad, Phys. Rev. B **67**, 155402 (2003).
[11] V. B. Shikin, JETP **33**, 387 (1971).
[12] S. A. Jackson and P. M. Platzman, Phys. Rev. B **24**, 499 (1981).